JOURNAL OF SOLID STATE CHEMISTRY 24, 389–394 (1978)

Magnetic Structure of the Low Temperature Antiferromagnetic Phase of V_2O_3*

H. KUWAMOTO, WILLIAM R. ROBINSON, AND J. M. HONIG

Department of Chemistry, Purdue University, West Lafayette, Indiana 47907

Received September 26, 1977

Using a magnetic space group analysis, V_2O_3 has been shown to have the $(A_g)_a$–G_b–$(A_g)_c$-type spin structure, which must be explained by both competitive metal–metal and metal–oxygen interactions. The spin orientation is analyzed in terms of the contribution provided by the magnetic anisotropy energy in V_2O_3.

Introduction

Numerous investigations (*1*) have shown that a sharp semiconductor–metal transition occurs in V_2O_3 in the temperature region 150–170°K and that an anomalous change in physical properties of V_2O_3 is encountered over the broad temperature range of 350–600°K. The low temperature transition is accompanied by a crystallographic change from monoclinic to rhombohedral symmetry (*2*). By contrast, the high temperature transition proceeds without change of the rhombohedral lattice symmetry (*3*). Relatively little attention has been devoted to the low temperature transition and to lattice properties of the monoclinic V_2O_3 phase. Earlier investigations involving neutron diffraction (*4*), magnetic susceptibility studies (*5*), Mössbauer measurements (*6*), and nuclear magnetic resonance (*7*), yielded conflicting evidence on whether monoclinic V_2O_3 exhibits magnetic spin order. However, the work by Moon (*8*) and Heidemann (*9*), using spin–flip polarized neutron scattering techniques, showed conclusively that all V atoms in planes perpendicular to the $[010]_m$ direction of the monoclinic phase are ferromagnetically aligned, while adjacent planes are coupled antiferromagnetically. No attempts appear to have been made to interpret the spin structure of the low temperature phase on the basis of phenomenological considerations; we have therefore undertaken this task.

* Research supported under NSF–MRL Grant DMR 76-00889.

Spin Configuration as Interpreted by Magnetic Space Groups

The following analysis is based on the procedure by Bertaut (*10*) for the magnetic space group appropriate to monoclinic V_2O_3. Dernier and Marezio (*11*) have reported the crystal structure and atomic positions of the low temperature, monoclinic, antiferromagnetic phase (Fig. 2) using the space group $I2/a$ suggested by McWhan and Remeika (*12*). Aside from the identity, the following independent symmetry operations of $I2/a$ superpose the crystal on itself: (i) rotations about the twofold axis $2b$ ($a = \frac{1}{2}$, $c = \frac{1}{2}$); (ii) inversion about the origin i ($a = 0$, $b = 0$, $c = 0$); and (iii) translation–rotation about the twofold screw axis $\tilde{2}b$ ($a = \frac{1}{2}$, $c = \frac{1}{2}$). Other, equivalent symmetry operations could have

0022–4596/78/2434–0389$02.00/0

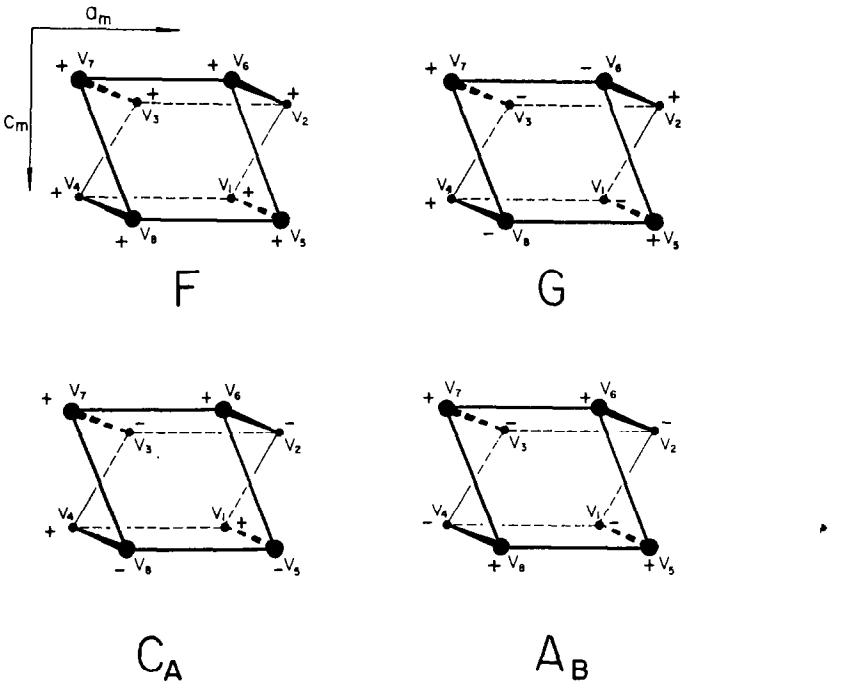

FIG. 1. Conventional basis configurations for spin alignments in monoclinic V_2O_3. The geometric figures indicate relative V_i positions. The + and − signs are to be interpreted in terms of components, as explained in the Text. The figures shown here represent one of several sets for different spin-up (+) and spin-down (−) assignments at the indicated vertices. For C_B, C_C configurations the linear chains run along the b_m and c_m unit cell axes, respectively, where b_m is perpendicular to both a_m and c_m. For A_A, A_C configurations the ferromagnetic planes are bounded by the $(b_m c_m)$ and $(a_m b_m)$ axes, respectively. Front face, $(020)_m$ plane, contains atoms V_5–V_8; rear face, $(010)_m$ plane, contains atoms V_1–V_4.

been used, but those introduced above are convenient.

The "basis functions" on which the above operations are to be performed are the conventional configurations *F, G, C,* and *A* (*10*), one set of which is shown in Fig. 1. These four groupings refer, respectively, to the ferromagnetic, nearest neighbor antiferromagnetic, linear ferromagnetic, and layer-type antiferromagnetic-type spin alignments on the lattice (in this case, vanadium) sites. The vertices in the front face of Fig. 1 represent vanadium sites (not vertices of the unit cell) in the $(020)_m$ plane of V_2O_3; those on the back face are V sites in the $(010)_m$ plane of V_2O_3. Attention is directed to the numbering of the V units which is indicated in Fig. 2 and explained in the caption of Fig. 1.

Eight distinct configurations of spin arrangements must be considered: those shown in Fig. 1 and additional sets (C_B, C_C, A_A, A_C) which correspond to different dispositions of "up" and "down" spins on the vertices of the *C* and *A* configurations as explained in the figure caption. All of these are to be understood as applying to the spin components. For example, the representation for site V_2 in Fig. 1 indicates that for the *F* and *G* configurations the V_2 atom on that site has positive spin components directed along the $\hat{a}_m$, $\hat{b}_m$, $\hat{c}_m$ directions while for the configurations C_A and A_B, V_2 has negative spin components along these axes.

One now operates on each of the magnetic symmetry structural units (basis functions) with each of the symmetry operations men-

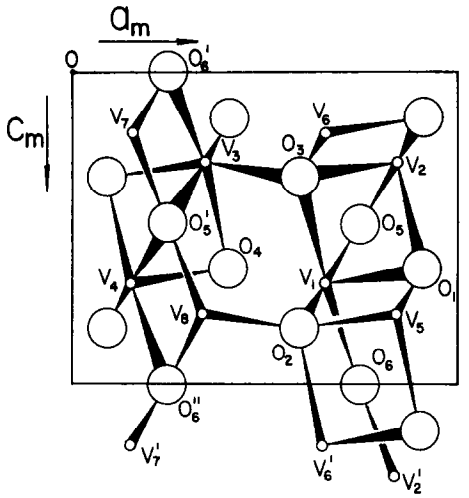

FIG. 2. A portion of the unit cell of monoclinic V_2O_3. V_1–V_4 are in the $(010)_m$ plane, V_5–V_8 in the $(020)_m$ plane. Note the numbering scheme. O designates the origin relative to which the symmetry operations are carried out. Small circles represent V atoms, large circles, O atoms.

tioned earlier, thereby interchanging spins on various equivalent sites. As expected, these interchange operations either leave a given spin component on equivalent sites unaltered, or else a sign change occurs. The results of these operations are displayed in Table I: here the entries + or − show that under the operation and for the component indicated in the heading, the spins remain unaltered or reverse sign. For example, when the operation $2b$ is performed on configuration F, spin components along a and c change in sign, but those along b do not; hence, the − + − sequence on the top left of the Table. In arriving at the results of Table I, it should be noted that spin angular momentum is represented as a pseudovector $\mathbf{r} \times \mathbf{p}$; hence, the inversion process does not change spin direction, whereas rotation about an axis perpendicular to the spin alignment does.

In Table II are summarized the eight sets of representations Γ_l appropriate to the transformation of the basis functions, under the symmetry operations described earlier. This is equivalent to the problem of distributing + and − signs among the operations $2b$, i, $\tilde{2}b$. For example, for Γ_6, the (− + −) designations refer in that order to the overall results of the $2b$, i, and $\tilde{2}b$ operations. This sequence is matched by the spin components along a of the basis function F; i.e. F_a. As seen from Table I, when the $2b$, i, $\tilde{2}b$ operations are carried out on the a component of the F magnetic symmetry structure, one recovers the values $-F_a$, $+F_a$, $-F_a$, respectively. No other basis function with spin components along a transforms in this particular manner, although the C_B basis with spin components along b, $(C_B)_b$, and the F basis with components along c, F_c, do. Other entries in Table II are constructed similarly; the corresponding magnetic ordering may (but need not necessarily) occur. Table II summarizes all possible spin orderings that could be encountered in any monoclinic lattice of

TABLE I

RESULTS OF SYMMETRY OPERATIONS ON THE BASIS FUNCTION COMPONENTS

	Operation $2b$			Operation i			Operation $\tilde{2}b$		
	Components			Components			Components		
Vector	a	b	c	a	b	c	a	b	c
F	−	+	−	+	+	+	−	+	−
G	+	−	+	+	+	+	−	+	−
C_A	+	−	+	−	−	−	+	−	+
C_B	+	−	+	+	+	+	+	−	+
C_C	−	+	−	−	−	−	−	+	−
A_A	−	+	−	−	−	−	+	−	+
A_B	−	+	−	+	+	+	+	−	+
A_C	+	−	+	−	−	−	−	+	−

TABLE II

REPRESENTATIONS OF BASIS FUNCTION COMPONENTS

	a	b	c
$\Gamma_1(+++)$	$(C_B)_a$	F_b	$(C_B)_c$
$\Gamma_2(++-)$	G_a	$(A_B)_b$	G_c
$\Gamma_3(+-+)$	$(C_A)_a$	$(C_C)_b$	$(C_A)_c$
$\Gamma_4(-++)$	$(A_B)_a$	G_b	$(A_B)_c$
$\Gamma_5(+--)$	$(A_C)_a$	$(A_A)_b$	$(A_C)_c$
$\Gamma_6(-+-)$	F_a	$(C_B)_b$	F_c
$\Gamma_7(--+)$	$(A_A)_a$	$(A_C)_b$	$(A_A)_c$
$\Gamma_8(---)$	$(C_C)_a$	$(C_A)_b$	$(C_C)_c$

$I2/a$ symmetry. As far as is known to the writers such a tabulation has not been constructed before.

Neutron diffraction studies (*8*, *9*) have established that V_2O_3 is a layer-type antiferromagnet whose spins are ferromagnetically aligned in the $(020)_m$ planes, which themselves are antiferromagnetically coupled. According to Table II and Fig. 1 the appropriate representations for such a configuration can only be $\Gamma_4(- + +)$, which involves the $(A_B)_a$–G_b–$(A_B)_c$-type spin alignment. Three-dimensional ferromagnetic ordering is precluded in V_2O_3 because the F_i components in Table II occur only in conjunction with basis functions other than the A type. The G_b-type ordering which is permitted by the $\Gamma_4(- + +)$ representation is, in fact, consistent with Moon's data (*8*), though he obtained as good a fit to his data without requiring the V spins to have any components along the b axis. Thus, G-type spin ordering along the b direction, if present, is weak.

Indirect Exchange Interaction

The mechanism of the superexchange interaction was first proposed by Kramers (*13*); Anderson (*14*) investigated the details of this process. Semiempirical rules for the superexchange interaction effects have been discussed by Goodenough (*15*) and enunciated by Kanamori (*16*). An attempt was made to apply these concepts to the case of monoclinic V_2O_3.

The spin Hamiltonian for V_2O_3 may be written (*17*) as follows:

$$H = \sum_{j>k} \{J_{jk} S_j \cdot S_k + S_j \cdot K_{jk} \cdot S_k\} + \sum_j DS_{jz}^2. \quad (1)$$

The first term represents the superexchange interaction, the second term accounts for the dipolar effects, and the third term represents the single-ion anisotropy due to spin–orbit interactions.

We first attempted to rationalize the observed spin ordering in monoclinic V_2O_3 on the basis of the first term, with $J_{jk} = -b^2J(p, d)/\Delta E^2$, where b is the transfer integral connecting a vanadium atom to the nearest neighbor oxygen, ΔE is the energy difference involved in the electron transfer, and $J(p, d)$ is the appropriate exchange integral. We found it impossible to force the observed antiferromagnetic coupling of ferromagnetic layers in V_2O_3 by this mechanism. This most probably indicates that overlap between vanadium e_π and a_1 orbitals with oxygen p orbitals is too large in V_2O_3 for second-order perturbation theory to be applicable, and further, that these contributions are in competition with the direct metal–metal interactions discussed by Goodenough (*18*) and reviewed elsewhere (*19*). Thus, we adopt Goodenough's explanation of antiferromagnetic ordering (*18*), with the modification that the energy levels, disposition of bands, and their widths are strongly affected by metal–oxygen interactions which occur in parallel with the direct metal–metal bonding. A quantitative treatment of this type for monoclinic V_2O_3 has recently been supplied by Ashkenazi and Weger (*20*) and by Castellani *et al.* (*21*), on the basis of detailed band structure calculations, in which electron correlations and polarizations are taken into account. These analyses show that in the vicinity of the Fermi level the valence bands are of the order of 0.8 eV in width, separated by a gap of approximately 0.2 eV from higher lying conduction bands. In these circumstances the simple superexchange formalism cannot be expected to apply. These findings support earlier speculations (*22*), based on thermoelectric power measurements, that the monoclinic phase is an insulator characterized by an itinerant rather than a localized charge carrier regime.

Magnetic Interactions

Both the experimental work and the theoretical analysis shows that the spin moments of vanadium are lying within a_m–c_m planes of the monoclinic phase of V_2O_3. We

seek to interpret the orientation of the spins in these planes relative to the short V–V distance in the $(010)_m$ planes [for example, V_1–V_2 in Fig. 2] which defines the hexagonal c_H axis direction in rhombohedral V_2O_3. In conformity with general practice we utilize the last two terms in Eq. (1) to determine the spin orientations in an itinerant antiferromagnet.

We turn first to the central dipolar interaction term which may be rewritten as

$$E_d = -\sum_j \frac{1}{r_{ij}^3}\left\{m_i \cdot m_j - 3\,\frac{(m_i \cdot r_{ij})(m_j \cdot r_{ij})}{r_{ij}^2}\right\}, \quad (2)$$

where r_{ij} is the separation between V atoms located on sites i and j and m_i is the dipole moment associated with the spin on site i.

In what follows we wish merely to demonstrate that this contribution is small compared to the anisotropy energy associated with the last term in Eq. (1). For this purpose it suffices to restrict the summation in Eq. (2) to nearest neighbors of atom V_i. This yields the approximate value

$$E_d \approx -0.048 \cos 2\theta - 0.039 \sin 2\theta \ (\mathrm{cm}^{-1}) \quad (3)$$

where θ is the canting angle of the spin in the a_m–c_m plane relative to the former hexagonal c axis. Extension of the summation to second, third, and higher order neighbor shells is necessary to obtain a more exact expression, but it is very unlikely that the results so obtained would alter the qualitative conclusions reached below.

We next turn to the third term in Eq. (1). When the anisotropic energy term is reexpressed in terms of θ, one obtains

$$E_a = DS(S - \tfrac{1}{2}) \cos^2\theta \approx 4.17 \cos^2\theta \ (\mathrm{cm}^{-1}) \quad (4)$$

in which the value $D = 8.34\ \mathrm{cm}^{-1}$, obtained from paramagnetic resonance measurements (*23*) on V-doped Al_2O_3, was introduced. The above can serve only as an order-of-magnitude estimate for E_a, but is probably correct to the extent of showing that E_a significantly exceeds E_d. As a first approximation, one may thus assume that the spin direction in the a_m–c_m plane is determined by the dependence of E_a on θ, which exhibits a minimum in E_a for θ at right angles to the c_H axis. Experimentally, a canting angle of 71° has been reported (*8*). Thus, the basic features of the experimental investigations on spin alignments in V_2O_3 have been reasonably well accounted for, but a more sophisticated analysis would be required for a refined interpretation.

References

1. See J. M. Honig and L. L. Van Zandt, *in* "Annual Review of Materials Science" (R. A. Huggins, Ed.) Vol. 5, p. 225, Annual Reviews Inc., Palo Alto, Calif. (1975).
2. E. P. Warekois, *J. Appl. Phys.* **31**, 3465 (1960).
3. D. B. McWhan and J. P. Remeika, *Phys. Rev. B* **2**, 3734 (1970). W. R. Robinson, *Acta Crystallogr. B* **31**, 1153 (1975). C. E. Rice and W. R. Robinson, *Phys. Rev. B* **8**, 3655 (1976).
4. A. Paoletti and S. J. Pickart, *J. Chem. Phys.* **32**, 308 (1960). H. Kendrick, A. Arrott, and S. A. Werner, *J. Appl. Phys.* **39**, 585 (1968).
5. D. J. Arnold and R. W. Mires, *J. Chem. Phys.* **48**, 2231 (1968).
6. G. K. Wertheim, J. P. Remeika, H. J. Guggenheim, and N. D. Buchanan, *Phys. Rev. Lett.* **25**, 94 (1970).
7. A. C. Gossard, D. B. McWhan, and J. P. Remeika, *Phys. Rev. B* **2**, 3762 (1970).
8. R. M. Moon, *Phys. Rev. Lett.* **25**, 527 (1970).
9. A. Heidemann, *Z. Phys.* **238**, 208 (1970).
10. W. C. Koehler, E. O. Wollan, and M. K. Wilkinson, *Phys. Rev.* **118**, 58 (1960). E. F. Bertaut, *in* "Magnetism" (G. T. Rado and H. Suhl, Eds.), Vol. 1, p. 149, Academic Press, New York (1963).
11. P. D. Dernier and M. Marezio, *Phys. Rev. B* **2**, 3771 (1970).
12. D. B. McWhan and J. P. Remeika, *Phys. Rev. B* **2**, 3734 (1970).
13. H. A. Kramers, *Physica* **1**, 182 (1934).
14. P. W. Anderson, *Phys. Rev.* **79**, 350 (1950).
15. J. B. Goodenough, *Phys. Rev.* **100**, 564 (1955).
16. J. Kanamori, *J. Phys. Chem. Solids* **10**, 87 (1959).
17. A. Abragam and M. H. L. Pryce, *Proc. Roy. Soc. Ser. A* **205**, 135 (1951).
18. J. B. Goodenough, *in* "Proc. 10th Int. Conf. on Physics of Semiconductors, Boston (1970)" (S. P. Keller, J. C. Hensel, and F. Stern, Eds.), pp. 304 ff.,

USAFC, NTIS, NBS, U.S. Dept. of Commerce, Springfield, Va. (1970).

19. R. W. VEST AND J. M. HONIG, *in* "Electrical Conductivity of Ceramics" (N. M. Tallan, Ed.), Part B, pp. 343 ff., Marcel Dekker, New York (1974).
20. J. ASHKENAZI AND M. WEGER, *Advan. Phys.* **22**, 207 (1973); *J. Phys.* (*Paris*) **37**, C4–189 (1976).
21. C. CASTELLANI, C. R. NATOLI, AND J. RANNINGER, *J. Phys.* (*Paris*) **37**, C4–199 (1976).
22. J. E. KEEM AND J. M. HONIG, *Phys. Status Solidi* **(a) 28**, 335 (1975).
23. A. GAVAIX, A. VASSON, A. M. VASSON, C. A. BATES, AND P. STEGGLES, *J. Phys. Chem. Solids* **37**, 1051 (1976).